0013-7227/07/$15.00/0
Printed in U.S.A.

Endocrinology 148(10):5088–5094

doi: 10.1210/en.2007-0701

Nesfatin-1: Distribution and Interaction with a G Protein-Coupled Receptor in the Rat Brain

G. Cristina Brailoiu, Siok L. Dun, Eugen Brailoiu, Saadet Inan, Jun Yang, Jaw Kang Chang, and Nae J. Dun

Department of Pharmacology (G.C.B., S.L.D., E.B., S.I., N.J.D.), Temple University School of Medicine, Philadelphia, Pennsylvania 19140; and Phoenix Pharmaceuticals, Inc. (J.Y., J.K.C.), Burlingame, California 94010

Nesfatin-1 is a recently identified satiety molecule detectable in neurons of the hypothalamus and nucleus of solitary tract (NTS). Immunohistochemical studies revealed nesfatin-1-immunoreactive (irNEF) cells in the Edinger-Westphal nucleus, dorsal motor nucleus of vagus, and caudal raphe nuclei of the rats, in addition to the hypothalamus and NTS reported in the initial study. Double-labeling immunohistochemistry showed that irNEF cells were vasopressin or oxytocin positive in the paraventricular and supraoptic nucleus; cocaine-amphetamine-regulated transcript or tyrosine hydroxylase positive in arcuate nucleus; cocaine-amphetamine-regulated transcript or melanin concentrating hormone positive in the lateral hypothalamus. In the brainstem, irNEF neurons were choline acetyltransferase positive in the Edinger-Westphal nucleus and dorsal motor nucleus of vagus; tyrosine hydroxylase positive in the NTS; and 5-hydroxytryptamine positive in the caudal raphe nucleus. The biological activity of rat nesfatin-1 (1–82) (100 nM) was assessed by the Ca^{2+} microfluorometric method. Nesfatin-1 elevated intracellular Ca^{2+} concentrations $[Ca^{2+}]_i$ in dissociated and cultured hypothalamic neurons. The response was prevented by pretreating the cells with pertussis toxin (100 nM) or Ca^{2+}-free solution and by a combination of the L-type and P/Q-type calcium channel blocker verapamil (1 μM) and omega-conotoxin MVIIC (100 nM). The protein kinase A inhibitor KT 5720 (1 μM) suppressed nesfatin-1-induced rise in $[Ca^{2+}]_i$. The result shows that irNEF is distributed to several discrete nuclei in the brainstem, in addition to the hypothalamus and NTS reported earlier, and that the peptide interacts with a G protein-coupled receptor, leading to an increase of $[Ca^{2+}]_i$, which is linked to protein kinase A activation in cultured rat hypothalamic neurons. (*Endocrinology* 148: 5088–5094, 2007)

FEEDING, ONE OF the most basic needs common to all animals, is a complex behavior orchestrated by a multitude of signaling molecules released from central and peripheral neurons and/or cells. Signaling molecules including ghrelin, orexins, adiponectin, agouti-related peptide, and cocaine-amphetamine regulated transcript peptide that prompt or suppress feedings, have been identified in the last few years (1–5). Nesfatin-1, an amino-terminal fragment derived from NEFA/nucleobindin 2 (NUCB2), is a recently identified satiety molecule (6). Immunohistochemical studies show that in the rat nesfatin-1-immunoreactivity (irNEF) is expressed in several discrete nuclei of the hypothalamus including the paraventricular (PVN) and supraoptic (SO) nucleus, the arcuate nucleus (Arc), the lateral hypothalamic area, and the zona incerta (6). In addition to the hypothalamus, irNEF is detectable in neurons of the nucleus of solitary tract (NTS) (6). This study had as its first aim the characterization of the phenotype of irNEF neurons in the hypothalamus and NTS as well as the newly identified areas by double-immunolabeling the sections with nesfatin-1 antiserum and antiserum to putative transmitters/enzymes known to express in respective areas.

Nesfatin-1 injected intracerebroventricularly to the rats reduced body weight in a dose-dependent manner, whereas injection of the antisense morpholino oligonucleotide against the gene encoding nucleobindin 2 increased body weight (6). Central administration of α-MSH elevated NUCB2 gene expression in the PVN, and prior administration of the melanocortin 3/4 receptor antagonist SHU9119 eliminated the nesfatin-1-induced satiety in rats, implying that a component of nesfatin-1 signaling pathway involves melanocortin (6). The receptor pharmacology and signaling mechanism directly associated with the action of nesfatin-1, however, has not been explored. With few exceptions, peptides including satiety and antisatiety molecules signal through G protein-coupled receptors. It is therefore hypothesized that nesfatin-1 interacts with a G protein-coupled receptor. The second aim was to explore the pharmacological property of the putative receptor or binding site, using Ca^{2+} flux as an indicator.

Materials and Methods

Adult male and female Sprague Dawley rats, weighing 250–275 g (Ace Animals Inc., Boyertown, PA), were used in this study, except in the series of experiments in which Ca^{2+} measurements were made from dissociated hypothalamic neurons harvested from 1- to 3-d-old rats. Animal protocols were reviewed and approved by the Institution Animal Care and Use Committee.

First Published Online July 12, 2007

Abbreviations: AGRP, Agouti-related peptide; Arc, arcuate nucleus; $[Ca^{2+}]_i$, intracellular Ca^{2+} concentration; CART, cocaine-amphetamine-regulated transcript antiserum; ChAT, choline acetyltransferase; DA, dorsal hypothalamic area; DMNV, dorsal motor nucleus of vagus; EW, Edinger-Westphal; irNEF, nesfatin-1 immunoreactivity; LH, lateral hypothalamic area; MCH, melanin-concentrating hormone antiserum; NPY, neuropeptide Y; NTS, nucleus of solitary tract; OT, oxytocin; POMC, proopiomelanocortin; PVN, paraventricular nucleus; ROb, raphe obscurus; RPa, raphe pallidus; SO, supraoptic nucleus; SOR, supraoptic retrochiasmatic nucleus; TH, tyrosine hydroxylase; VP, vasopressin.

***Endocrinology* is published monthly by The Endocrine Society (http://www.endo-society.org), the foremost professional society serving the endocrine community.**

Immunohistochemistry

Animals anesthetized with urethane (1.2 g/kg, ip) were intracardially perfused with 0.1 M PBS followed by 4% paraformaldehyde/0.2% picric acid in PBS. Brains were removed, postfixed for 2 h, and stored in 30% sucrose/PBS solution overnight.

In single staining, tissues were processed for irNEF by the avidin-biotin complex procedure (7). The brain was embedded in agar and coronal sections of 50 μm thickness were prepared with the use of a Vibratome. Tissues were first treated with 3% H_2O_2 to quench endogenous peroxidase, washed several times, blocked with 10% normal goat serum, and incubated in nesfatin-1 antiserum (1:1000 dilution), which was a rabbit polyclonal raised against the rat nesfatin-1 N terminus (1–82) (Phoenix Pharmaceuticals, Inc., Burlingame, CA). Nesfatin-1 antiserum cross-reacts 100% with rat nesfatin-1 (1–82) and does not cross-react with the following peptides: nesfatin-1 (1–45, human), nesfatin-1 (47–82, human), agouti-related peptide (83–132, human), α-MSH, orexin A (human, rat, mouse), neuropeptide Y (rat), ghrelin (rat, mouse), and obestatin (rat, mouse). After thorough rinsing, sections were incubated in biotinylated antirabbit IgG (1:200 dilution; Vector Laboratories, Burlingame, CA) for 2 h and rinsed with PBS and incubated in avidin-biotin complex solution for 1.5 h (1:100 dilution; Vector Laboratories). After several washes in Tris-buffered saline, sections were developed in 0.05% diaminobenzidine/0.001% H_2O_2 solution and washed for at least 2 h with Tris-buffered saline. Sections were mounted on slides with 0.25% gel alcohol, air dried, dehydrated with absolute alcohol followed by xylene, and coverslipped with Permount.

For control experiments, sections were processed with nesfatin-antiserum preabsorbed with the rat nesfatin-1 peptide (1–82) (10 μg/ml) overnight or by substituting nesfatin-1 antiserum with normal rabbit serum.

In the case of double-labeling experiments, hypothalamic and medullary sections were first blocked with normal goat serum (1:10 in PBS, 0.5% BSA, 0.4% Triton X-100) and then incubated with nesfatin-1 antiserum (1:500 dilution). After several washes with PBS, sections were incubated with biotinylated antirabbit IgG (1:50, Vector Laboratories), washed with PBS, and incubated with fluorescein avidin D. After rinsing with PBS, hypothalamic sections were blocked with normal donkey serum (Jackson ImmunoResearch Laboratories, Inc., West Grove, PA) and incubated with oxytocin (OT) antibody (1:1000 dilution, a monoclonal from Chemicon, Temecula, CA), vasopressin (VP) antiserum (1:1500 dilution, a guinea pig polyclonal from Chemicon), tyrosine hydroxylase (TH) antibody (1:750, a mouse monoclonal from Chemicon), neuropeptide Y (NPY) antiserum (1:750, a sheep polyclonal from Chemicon), cocaine-amphetamine-regulated transcript antiserum (CART; 1:500; Phoenix Pharmaceuticals), melanin-concentrating hormone antiserum (MCH; 1:300; Phoenix Pharmaceuticals), and proopiomelanocortin (POMC; 1:400; Phoenix Pharmaceuticals) antiserum. Medullary sections were incubated with choline acetyltransferase (ChAT) antiserum (1:200; a guinea pig polyclonal from Bachem BioSciences Inc., King of Prussia, PA), 5-HT antiserum (1:300, a goat polyclonal from Chemicon), TH antiserum, or POMC antiserum for 48 h in a cold room. Tissues were then incubated in appropriate IgG Texas Red antibodies, washed with PBS, and mounted in Citifluor and coverslipped. Sections were examined under a confocal scanning laser microscope (TCS SL; Leica Microsystems Inc., Exton, PA) with excitation/emission wavelengths set to 488/520 nm for fluorescein isothiocyanate and 543/620 nm for Texas Red in the sequential mode.

Neuronal cell culture

Cells were isolated from the hypothalamus of postnatal 1- to 3-d-old rats by enzymatic digestion with 0.5 mg papain per 100 mg tissue (8). Cells were plated at a density of 10^3 cells/mm^2 in a Neurobasal-A medium, supplemented with 10% fetal calf serum, 2 mM glutamine, 100 U/ml penicillin, and 100 μg/ml streptomycin (Invitrogen, Carlsbad, CA), and maintained at 37 C in a humidified atmosphere with 5% CO_2. Glial cell growth was inhibited by the mitotic inhibitor cytosine β-arabino furanoside (1 μM) (Sigma, St. Louis, MO). Neurons were cultured for 5 d. Cells were transferred to a medium without fetal serum 12 h before Ca^{2+} measurements.

Cytosolic Ca^{2+} concentrations

Cytosolic Ca^{2+} measurements were performed as described previously (8, 9). Cells were incubated with 5 μM fura-2AM (Molecular Probes, Eugene, OR) in Hanks' balanced salt solution (HBSS) at room temperature for 45 min in the dark, washed three times with dye-free buffer, and then incubated for another 45 min to allow for complete deesterification of the dye. Coverslips were subsequently mounted in a custom-designed bath on the stage of an Eclipse TE 2000-U (Nikon, Tokyo, Japan) inverted microscope equipped with a CCD camera (Roper Scientific, Tucson, AZ). Cells were routinely superfused with HBSS at a flow rate of 1 ml/min. Fura-2 fluorescence (emission = 510 nm), after alternate excitation at 340 and 380 nm, was acquired at a frequency of 0.33 Hz. Images were acquired and analyzed using Metafluor software. For Ca^{2+}-free experiments, HBSS without Ca^{2+} and supplemented with 2.5 mM EGTA was used.

Statistical analysis

In calcium measurement experiments, statistical significance between groups was tested using one-way ANOVA followed by Bonferroni test, $P < 0.05$ being considered significant.

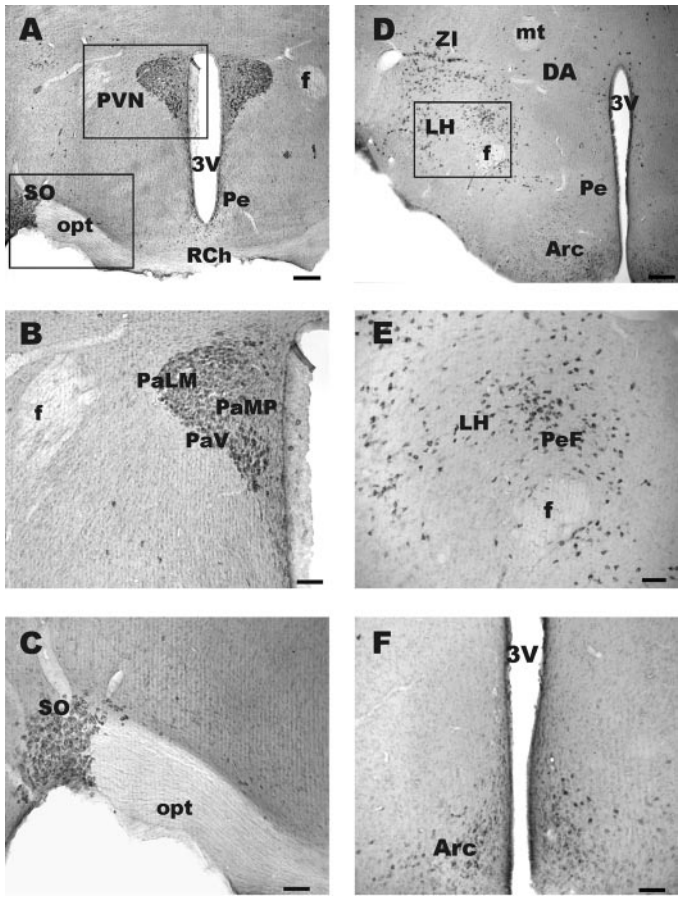

FIG. 1. Hypothalamic sections labeled with nesfatin-1 antiserum. A, Numerous irNEF cells are present in the PVN and SO; few cells are scattered in the periventricular hypothalamic nucleus (Pe) and retrochiasmatic nucleus (RCh). B, A higher magnification of the area outlined in A, in which numerous irNEF neurons are seen in the PVN subdivisions: lateral magnocellular part (PaLM), ventral part (PaV), and medial parvicellular part (PaMP). C, Numerous irNEF cells are seen in the SO. D, Hypothalamus at the level of median eminence in which irNEF neurons are detected in the Arc, LH, zona incerta (ZI), around the fornix (f), and in the DA. E, A higher magnification of area outlined in D, in which labeled cells are present in the LH, and perifornical nucleus (PeF). F, irNEF cells are seen in the arcuate nucleus. 3V, Third ventricle; mt, mammilothalamic tract; opt, optic tract. *Scale bar*, A and D, 250 μm; B, C, E, and F, 100 μm.

Results

Immunohistochemistry

Single labeling results were obtained from four male and four female adult Sprague Dawley rats. In addition, brain tissues from two male rats were processed for double labeling. The pattern of distribution of irNEF cells was similar in male and female rats. In addition to the hypothalamus and NTS, irNEF neurons were noted in several areas not previously reported (6). A more extensive description of the distribution of irNEF neurons is therefore presented below.

Hypothalamus

Positively labeled cells were distributed to the PVN and SO; few cells were scattered in the periventricular hypothalamic nucleus and the retrochiasmatic nucleus (Fig. 1, A–C). Within the PVN, irNEF cells were concentrated in the lateral magnocellular part and ventral part (PaV), with fewer cells in the medial parvicellular part (Fig. 1, A and B). At the level of median eminence, numerous irNEF cells were noted in the lateral hypothalamic area (LH), zona incerta, perifornical nucleus, dorsal hypothalamic area (DA), and Arc (Fig. 1, D–F). At a more caudal level, irNEF neurons were distributed to the LH, subincertal nucleus, DA, and Arc as well as the dorsomedial nucleus, dorsal, ventromedial hypothalamic nucleus, and supraoptic retrochiasmatic nucleus (SOR) (Fig. 2, A and B). Overall, the distribution of irNEF neurons observed in the hypothalamus was similar to that reported earlier (6).

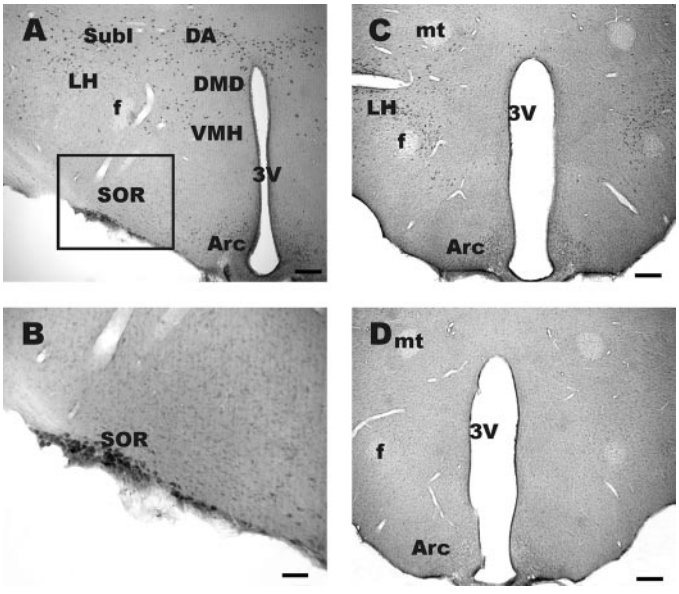

FIG. 2. Hypothalamic sections labeled with nesfatin-1 antiserum or nesfatin-1 antiserum preabsorbed with the peptide. A, A caudal hypothalamic section labeled with nesfatin-1 antiserum in which numerous irNEF cells are seen in the DA, subincertal nucleus (SubI), LH, dorsal part of the dorsomedial nucleus (DMD), ventromedial hypothalamic nucleus (VMH), Arc, and SOR. B, A higher magnification of the area outlined in A, in which strongly labeled cells are seen in SOR. C and D, Hypothalamic sections at similar level labeled with nesfatin-1 antiserum (C) or nesfatin-1 antiserum preabsorbed with nesfatin-1 peptide (10 μg/ml) overnight; labeled cells are not seen in D. 3V, Third ventricle; mt, mammilothalamic tract. *Scale bar*, A, C, and D, 250 μm; B, 100 μm.

Control studies

Hypothalamic or medullary sections processed with nesfatin-1 antiserum preabsorbed with the peptide (10 μg/ml) showed no labeled cells. A hypothalamic section labeled with nesfatin-1 antiserum showed numerous irNEF neurons in the LH, perifornical nucleus, and Arc (Fig. 2C), whereas positively labeled cells were not detected in an adjacent hypothalamic section processed with nesfatin-1 antiserum preabsorbed with the peptide overnight (Fig. 2D). Similarly, substitution of nesfatin-1 antiserum with normal rabbit serum resulted in no immunoreactivity in any of the sections examined.

Pons and medulla oblongata

Similar to an earlier report (6), irNEF cells were detected in the nucleus of solitary tract (Fig. 3, A and B). Moderately labeled cells could also be detected in the dorsal motor nucleus of vagus (10) (Fig. 3, A and B). In addition, the Edinger-Westphal (EW) nucleus contained irNEF neurons (Fig. 3C). Cells in the caudal raphe nuclei including the nucleus raphe obscurus (ROb) and raphe pallidus (RPa) expressed irNEF (Fig. 3D).

Double-labeling studies

Neurons in the PVN and SO contain VP or OT (11). Double labeling the hypothalamic sections with nesfatin-1 antiserum and VP antiserum or OT antiserum revealed that some of the irNEF neurons were VP positive and others were OT positive (Fig. 4, A1–A3, and B1–B3). Some of the neurons in the Arc contain the catecholaminergic neuron marker tyrosine hydroxylase (TH) (12, 13). Double labeling the hypothalamic sections with nesfatin-1 antiserum and TH antiserum

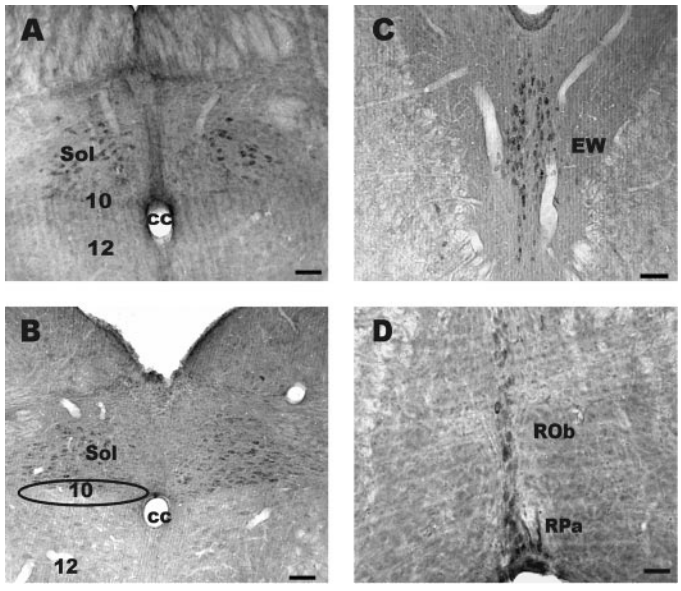

FIG. 3. Brainstem nuclei expressing irNEF. A and B, irNEF cells are detectable in the nucleus of the nucleus of solitary tract and dorsal motor nucleus of vagus (10); a cluster of moderately labeled irNEF cells can clearly be seen in 10, which is outlined but not in the hypoglossal nucleus (12). C, irNEF cells in the EW. D, irNEF neurons are seen in the ROb and RPa. cc, Central canal. *Scale bar*, A–C, 100 μm; D, 50 μm.

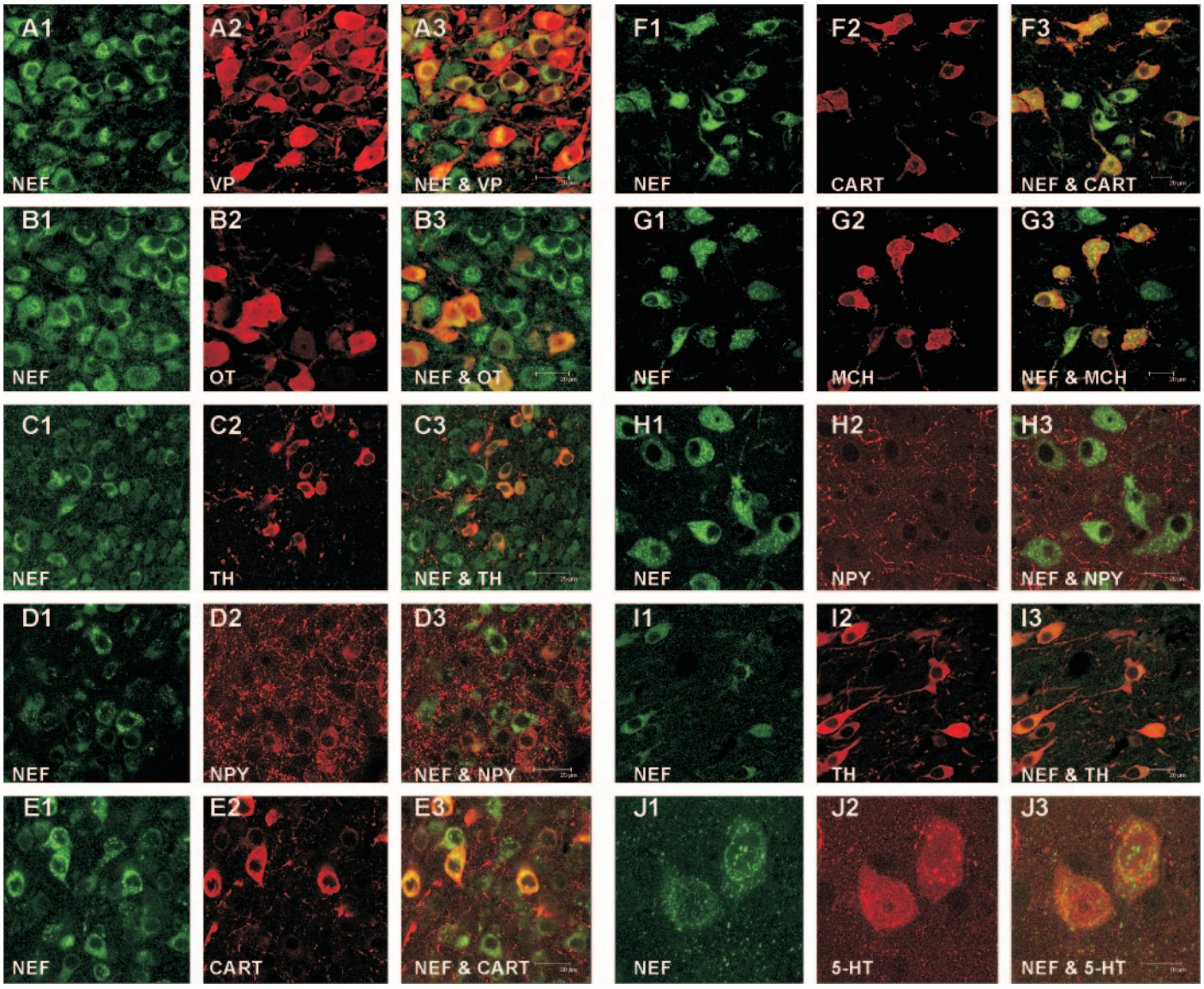

FIG. 4. Confocal images of rat hypothalamic and brainstem sections double labeled with nesfatin-1 and VP, OT, tyrosine hydroxylase, NPY, CART, MCH, or 5-HT antiserum. A1 and A2, irNEF and VP-positive cells are seen in the paraventricular hypothalamic nucleus. A3, A merged image of A1 and A2 in which several irNEF cells also express VP. B1 and B2, irNEF and OT-positive cells in the paraventricular hypothalamic nucleus. B3, A merged image of B1 and B2 in which a few irNEF cells are OT positive; the majority of irNEF cells are oxytocin negative. C1 and C2, irNEF neurons and TH-positive cells in the Arc. C3, A merged image of C1 and C2 in which several irNEF cells also contain TH. D1 and D2, irNEF neurons and NPY immunoreactivity in the Arc. D3, A merged image of D1 and D2 in which NPY-immunoreactive fibers are in close proximity to irNEF neurons. E1 and E2, irNEF neurons and CART-positive cells in the Arc. E3, A merged image of E1 and E2 in which several irNEF cells express CART immunoreactivity. F1 and F2, irNEF and CART-positive cells in the LH. F3, A merged image of F1 and F2 in which several irNEF cells are also CART positive. G1 and G2, irNEF and MCH-immunoreactive cells in the LH. G3, A merged image of G1 and G2 in which some irNEF cells also express MCH immunoreactivity. H1 and H2, irNEF neurons and NPY-positive cell processes in the LH. H3, A merged image of H1 and H2 in which NPY-positive fibers are seen in close vicinity of irNEF cells. I1 and I2, irNEF cells and TH cells in the NTS. I3, A merged image of I1 and I2 in which the majority of irNEF neurons were TH positive. J1 and J2, irNEF cells and 5-HT cells in the RPa nucleus. J3, A merged image of J1 and J2 in which irNEF neurons also express 5-HT. *Scale bar*, A1–A3, B1–B3, E1–E3, F1–F3, G1–G3, H1–H3, I1–I3, 20 μm; C1–C3 and D1–D3, 25 μm; J1–J3, 10 μm.

showed that in the Arc some of the irNEF cells exhibit TH immunoreactivity (Fig. 4, C1–C3). Whereas irNEF was not detectable in NPY-positive neurons, NPY-positive fibers were in close proximity to irNEF neurons in the Arc (Fig. 4, D1–D3) and PVN. Some irNEF cells from the Arc were also CART positive (Fig. 4, E1–E3) or POMC positive (not shown). In the lateral hypothalamic area, irNEF was found in neurons exhibiting CART immunoreactivity (Fig. 4, F1–F3) or MCH immunoreactivity (Fig. 4, G1–G3), whereas NPY-positive fibers were identified in the vicinity of irNEF neurons (Fig. 4, H1–H3).

With respect to the brainstem, double-labeling experiments showed that the majority of irNEF neurons were TH positive (Fig. 4, I1–I3) or POMC positive (not shown) in the NTS, and irNEF neurons in the dorsal motor nucleus of vagus (DMNV) and EW nucleus were ChAT positive (not

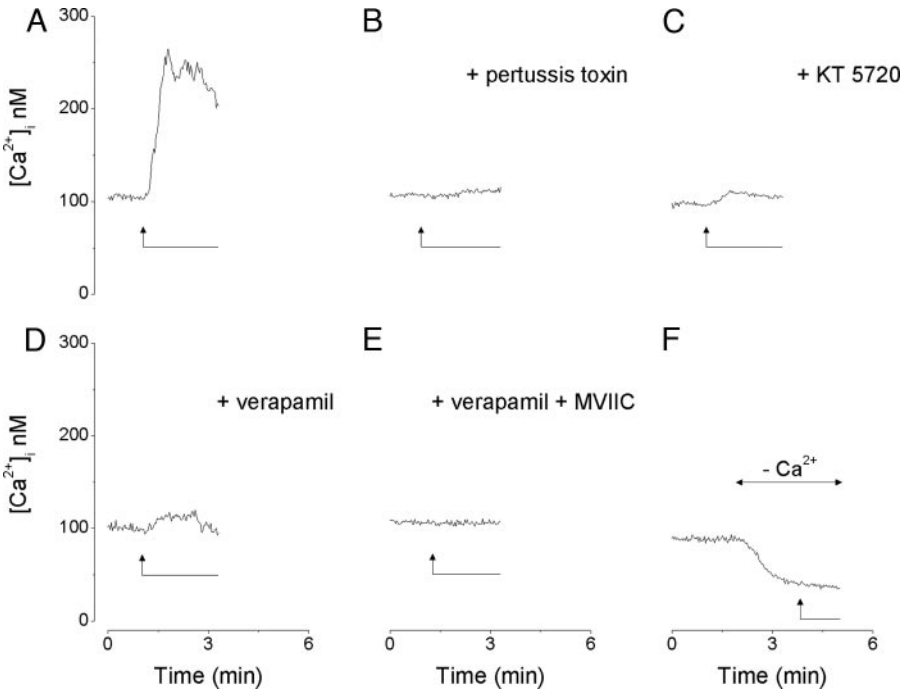

FIG. 5. Calcium responses induced by nesfatin-1 in rat hypothalamic neurons. A, Nesfatin-1 (100 nM, *arrow*) induced a fast increase in $[Ca^{2+}]_i$ followed by a plateau. B, Pretreatment with pertussis toxin (100 ng/ml, 1 h) prevented the increase in $[Ca^{2+}]_i$ by nesfatin-1. C and D, Pretreatment with KT 5720 (1 μM, 30 min) or verapamil (1 μM, 30 min) diminished the increase in $[Ca^{2+}]_i$ by nesfatin-1. E, Pretreatment with verapamil (1 μM, 30 min) and ω-conotoxin MVIIC (0.1 μM, 1 h) abolished the calcium response to nesfatin-1. F, Perfusion with Ca^{2+}-free saline for the duration indicated, prevented the increase in $[Ca^{2+}]_i$ by nesfatin-1. A–F, Examples of actual Ca^{2+} traces from six different hypothalamic neurons; *arrows* indicate the addition of nesfatin-1.

shown). Lastly, irNEF cells in the caudal raphe nuclei were 5-HT immunoreactive (Fig. 4, J1–J3).

Intracellular Ca^{2+} concentrations

The neuronal activity of nesfatin-1 was assessed by a change of intracellular calcium concentrations $[Ca^{2+}]_i$ in dissociated and cultured hypothalamic neurons. The basal $[Ca^{2+}]_i$ value of rat dissociated central neurons varied from 70 to 180 nM, which is in agreement with the concentration (30–200 nM) reported in mammalian central neurons (14). Nesfatin-1 (100 nM) by superfusion induced an elevation of $[Ca^{2+}]_i$ by 164 ± 3.6 nM in 11 of 87 hypothalamic neurons tested (Figs. 5A and 6). In 47 cells pretreated with pertussis toxin (100 ng/ml) for 1 h, nesfatin-1 caused no significant changes of $[Ca^{2+}]_i$, indicating that the peptide acts through $G_{i/o}$ protein coupled receptors (Figs. 5B and 6).

In Ca^{2+}-free saline supplemented with 2.5 mM EGTA, administration of nesfatin-1 had little or no effects on $[Ca^{2+}]_i$ in all 38 cells tested (Figs. 5F and 6), indicating that the rise in $[Ca^{2+}]_i$ is derived mainly from influx of Ca^{2+} through plasmalemmal calcium channels. Pretreatment of the hypothalamic neurons with the L-type Ca^{2+} channel blocker verapamil (1 μM, 30 min) produced an increase of $[Ca^{2+}]_i$ by only 38 ± 2.3 nM above the basal level in 8 cells tested (Figs. 5D and 6). Pretreating the cells with the N-type Ca^{2+} channel blocker ω-conotoxin GVIA (0.1 μM) and verapamil (1 μM, 30 min) suppressed the increase of $[Ca^{2+}]_i$ by nesfatin-1 to a similar degree as that caused by pretreatment of the cells with verapamil alone (n = 9; Fig. 6). Concomitant administration of verapamil and the P/Q Ca^{2+} channel blocker ω-conotoxin MVIIC (0.1 μM; 1 h) abolished the Ca^{2+} responses (n = 31; Figs. 5E and 6). Unexpectedly, the effect of nesfatin-1 on $[Ca^{2+}]_i$ was significantly reduced by pretreatment of the neurons with the specific protein kinase A blocker KT 5720 (1 μM) (Fig. 5C); the average increase of $[Ca^{2+}]_i$ was 24 ± 1.6 nM (n = 26) above the basal level in cells pretreated with KT 5720 (Fig. 6).

Discussion

Similar to the pattern of distribution first described by Oh-1 *et al.* (6) using immunohistochemistry and *in situ* hybridization, our result shows that irNEF cells are present in the hypothalamus and NTS. In addition, our result reveal several groups of irNEF neurons in the brainstem that were not reported earlier, namely the EW nucleus, DMNV, ROb, and RPa nuclei. Because the number of labeled cells in these nuclei is relatively small, they may have been overlooked in the early study (6). Double-labeling studies reveal a heterogeneous population of neurons expressing irNEF that are area specific. For example, irNEF is expressed in VP or OT cells of the PVN and SO and in TH-positive as well as CART-positive cells of the Arc. In the lateral hypothalamus, irNEF are colocalized with CART and MCH. In the brainstem, irNEF is expressed in ChAT-positive, thus cholinergic, neurons of the EW nucleus and DMNV; catecholaminergic neurons of the NTS; and serotoninergic cells of the caudal raphe nuclei.

Several lines of evidence suggest that nesfatin-1 may function as an anorexigenic peptide (6). Nesfatin-1 gene and protein are found in the hypothalamic nuclei known to be involved in feeding behaviors, food intake, body weight, and glucose homeostasis (15). The Arc is the major site in which leptin activates POMC and CART neurons but inhibits agouti-related peptide (AGRP) and NPY neurons (10, 16, 17). POMC/CART and AGRP/NPY neurons are distinct populations in the Arc (18). Double-labeling studies demonstrate that irNEF is expressed in CART-positive and POMC-positive but not NPY-positive neurons; instead, NPY-immunoreactive fibers appear to be in close proximity to irNEF neurons in the Arc, PVN, and LH. Because almost all CART neurons are found to contain POMC and vice versa (19), the colocalization of nesfatin-1 with both CART and

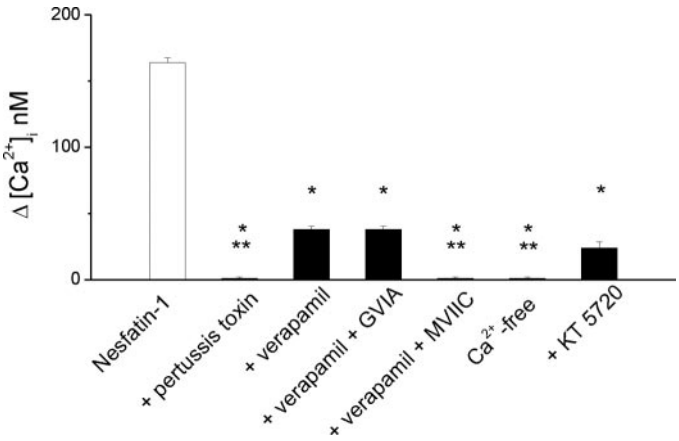

FIG. 6. Comparison of changes in Ca^{2+} induced by nesfatin-1 in different experimental conditions. Nesfatin-1 (100 nM) induced an increase of $[Ca^{2+}]_i$ by 164 + 3.6 nM (n = 11, *first column*), which was reduced by pretreatment with verapamil alone (1 μM, 30 min; n = 8) or in combination with ω-conotoxin GVIA (0.1 μM, 1 h; n = 9), and by pretreatment with KT 5720 (1 μM, 30 min; n = 26). The Ca^{2+} response to nesfatin-1 was abolished by pretreatment with pertussis toxin (100 ng/ml, 1 h; n = 47), verapamil, and ω-conotoxin MVIIC (0.1 μM, 1 h; n = 31) or by perfusion with Ca^{2+}-free saline (n = 38). *, Statistically significant difference ($P < 0.05$) as compared with nesfatin-1; **, statistically significant difference as compared with nesfatin-1 and verapamil, nesfatin-1 and verapamil + ω-conotoxin GVIA, nesfatin-1, and KT 5720.

POMC is not unexpected. Nesfatin-1 by intracerebroventricular injection was found not to affect the expression of genes encoding POMC, AGRP, and NPY in the Arc, suggesting a leptin-independent signaling (6). In the Arc, some of the irNEF are also TH positive; the latter belong to dopaminergic neurons of the tuberoinfundibular system, which regulates the secretion of prolactin (20, 21).

In the case of PVN and SO, irNEF neurons are found to overlap with VP or OT cells. CRH is also known to be localized in a population of VP and OT neurons (22). Nesfatin-1 injected intraventricularly did not significantly modify the expression of the gene encoding CRH (6), suggesting that CRH neurons may not be the primary target of nesfatin-1 in the hypothalamus.

The largest number of irNEF neurons is found in the LH, which contain a heterogeneous group of neurons expressing diverse transmitter phenotypes. Our result shows that in the lateral hypothalamic area some of the irNEF neurons exhibit CART or MCH immunoreactivity and are surrounded by NPY-positive fibers. Neurons in the LH are known to be closely associated with food intake, body weight, and other metabolic processes (23). The role of nesfatin-1 in this integrative circuitry subserving the ingestive behavior remains to be explored. The colocalization of nesfatin-1 with peptides having both stimulatory (MCH) and inhibitory (CART) effect on feeding is not without precedent because CART is also identified in POMC- and MCH-containing neurons (19).

In addition to the hypothalamus, irNEF neurons are noted in the NTS, as reported by Oh-I *et al.* (6). Double-labeling experiments demonstrate that irNEF neurons in the NTS contain TH, thus are catecholaminergic. In addition, irNEF neurons in the NTS expressed varying levels of POMC immunoreactivity. A large percentage of catecholaminergic neurons in the NTS projects to the PVN (24). As a corollary, irNEF neurons in the NTS send their axons to the PVN, in which the peptide may modulate the activity of PVN.

Three additional groups of irNEF neurons are identified in the brainstem, namely the EW nucleus, DMNV, and caudal raphe nuclei. Double-labeling studies show that irNEF neurons are ChAT positive in the EW nucleus and DMNV and 5-HT-positive in the caudal raphe nuclei. A large majority of neurons in the DMNV innervate the gastrointestinal tract (25). Viewed in this context, nesfatin-1 released from the vagus nerve may modify the activity of gastrointestinal tract, which is consistent with the notion that nesfatin-1 regulates ingestive behaviors. On the other hand, the functional significance of nesfatin-1 in neurons of the EW nucleus is not clear. The EW nucleus contains preganglionic parasympathetic neurons whose axons end in the ciliary ganglion, which in turn send their axons to the sphincter pupillae of the iris and the ciliary muscles of the eye. Other peptides known to be present in the EW nucleus, such as urocortin and CART, are involved in the regulation of feeding and response to stress (26, 27).

With respect to the caudal raphe nuclei, irNEF is present in some of the serotoninergic neurons of the RPa and ROb. In addition to projecting to the brainstem and spinal cord and participating in the regulation of motor and somatosensory functions (28, 29), some of the serotoninergic neurons are thought to be sympathetic premotor neurons with brown fat pads as their target sites (30, 31). Thus, nesfatin-1 via this sympathetic bulbospinal pathway may play a role in thermogenesis and related energy homeostasis.

Using Ca^{2+} flux as an index, our result suggests that nesfatin-1 interacts with a receptor with pharmacological characteristics of a G protein-coupled receptor in the cultured rat hypothalamic neurons. Nesfatin-1 induced an elevation of $[Ca^{2+}]_i$ characterized by a relatively fast rise followed by a plateau. The response is abolished by pertussis toxin, indicating the participation of a $G_{i/o}$ protein coupled receptor. Nesfatin-1-induced calcium increases were abolished in a Ca^{2+}-free medium, indicating that the peptide increases Ca^{2+} influx from the extracellular space. Results obtained with inhibitors specific for subtypes of Ca^{2+} channels indicate that the calcium channel activated by nesfatin-1 exhibits pharmacological characteristics of L and P/Q channels.

The specific protein kinase A inhibitor KT 5720 (32), which is plasma membrane permeable, has been previously demonstrated to be effective in neurons at the concentrations used in our study (33–35). Nesfatin-1-induced elevation of $[Ca^{2+}]_i$ was significantly reduced by KT 5720, suggesting an involvement of protein kinase A in nesfatin-1-induced Ca^{2+} responses in hypothalamic neurons. This is unexpected because activation of G_i is generally associated with a decrease of cAMP levels (36). One possible explanation is that one agonist can activate different pathways by switching receptor coupling between different G proteins (37). For example, nesfatin-1 may initially activate G_i and later switch to G_s stimulation. A sequential activation has been shown for G_s/G_i but not G_i/G_s (38). Consequently, this model may not be applicable to our observation. A recent observation by Dunn *et al.* (39), who measured concomitantly intracellular Ca^{2+}/cAMP levels and protein kinase A activity reveals that, in neonatal rat retinal explants, Ca^{2+} entry through plasmalemma but not Ca^{2+} release from internal sources activates cAMP production in seconds. Moreover, it has been

shown that activation of G_i induces a functional compartmentalization of protein kinase A signaling (40). Our interpretation is that nesfatin-1 activates spatiotemporary restricted Ca^{2+} and protein kinase A signaling, leading to a highly specific role in intracellular signaling cascade.

In summary, our result shows that in the rat nesfatin-1 is expressed in discrete populations of hypothalamic and brainstem neurons and that the peptide stimulates calcium influx in cultured hypothalamic neurons by interacting with a yet to be identified G protein-coupled receptor.

Acknowledgments

Received May 23, 2007. Accepted July 2, 2007.

Address all correspondence and requests for reprints to: G. Cristina Brailoiu, M.D., Department of Pharmacology, Temple University School of Medicine, 3420 North Broad Street, Philadelphia, Pennsylvania 19140. E-mail: gbrailou@temple.edu.

This work was supported by National Institutes of Health Grants NS18710 and HL51314 from the Department of Health and Human Services.

Disclosure Statement: All authors have nothing to declare.

References

1. **Kojima M, Hosoda H, Date Y, Nakazato M, Matsuo H, Kangawa K** 1999 Ghrelin is a growth-hormone-releasing acylated peptide from stomach. Nature 402:656–660
2. **Kristensen P, Judge ME, Thim L, Ribel U, Christjansen KN, Wulff BS, Clausen JT, Jensen PB, Madsen OD, Vrang N, Larsen PJ, Hastrup S** 1998 Hypothalamic CART is a new anorectic peptide regulated by leptin. Nature 393:72–76
3. **Ollmann MM, Wilson BD, Yang YK, Kerns JA, Chen Y, Gantz I, Barsh GS** 1997 Antagonism of central melanocortin receptors *in vitro* and *in vivo* by agouti-related protein. Science 278:135–138
4. **Qi Y, Takahashi N, Hileman SH, Patel HR, Berg AH, Pajvani UB, Scherer PE, Ahima RS** 2004 Adiponectin acts in the brain to decrease body weight. Nat Med 10:524–529
5. **Sakurai T, Amemiya A, Ishii M, Matsuzaki I, Chemelli RM, Tanaka H, Williams SC, Richardson JA, Kozlowski GP, Wilson S, Arch JR, Buckingham RE, Haynes AC, Carr SA, Annan RS, McNulty DE, Liu WS, Terrett JA, Elshourbagy NA, Bergsma DJ, Yanagisawa M** 1998 Orexins and orexin receptors: a family of hypothalamic neuropeptides and G protein-coupled receptors that regulate feeding behavior. Cell 92:573–585
6. **Oh-I S, Shimizu H, Satoh T, Okada S, Adachi S, Inoue K, Eguchi H, Yamamoto M, Imaki T, Hashimoto K, Tsuchiya T, Monden T, Horiguchi K, Yamada M, Mori M** 2006 Identification of nesfatin-1 as a satiety molecule in the hypothalamus. Nature 12:709–712
7. **Dun NJ, Dun SL, Wu SY, Förstermann U, Schmidt HH, Tseng LF** 1993 Nitric oxide synthase immunoreactivity in the rat, mouse, cat and squirrel monkey spinal cord. Neuroscience 54:845–857
8. **Dun SL, Brailoiu E, Wang Y, Brailoiu GC, Liu-Chen LY, Yang J, Chang JK, Dun NJ** 2006 Insulin-like peptide 5: expression in the mouse brain and mobilization of calcium. Endocrinology 47:3243–3248
9. **Brailoiu E, Churamani D, Pandey V, Brailoiu GC, Tuluc F, Patel S, Dun NJ** 2006 Messenger-specific role for nicotinic acid adenine dinucleotide phosphate in neuronal differentiation. J Biol Chem 281:15923–15928
10. **Elmquist JK, Bjorbaek C, Ahima RS, Flier JS, Saper CB** 1999 Distributions of leptin receptor mRNA isoforms in the rat brain. J Comp Neurol 395:535–547
11. **Rhodes CH, Morrell JI, Pfaff DW** 1981 Immunohistochemical analysis of magnocellular elements in rat hypothalamus: distribution and numbers of cells containing neurophysin, oxytocin, and vasopressin. J Comp Neurol 198:45–64
12. **Meister B, Hökfelt T, Steinbusch HWM, Skagerberg G, Lindvall O, Geffard M, Joh T, Cuello AC, Goldstein M** 1988 Do tyrosine hydroxylase-immunoreactive neurons in the ventro-lateral arcuate nucleus produce dopamine or only L-dopa? J Chem Neuroanat 1:59–64
13. **Van den Pol AN, Herbst RS, Powell JF** 1984 Tyrosine hydroxylase-immunoreactive neurons of the hypothalamus: a light and electron microscopic study. Neurosci 13:1117–1156
14. **Connor JA** 1986 Digital imaging of free calcium changes and of spatial gradients in growing processes in single, mammalian central nervous system cells. Proc Natl Acad Sci USA 83:6179–6183
15. **Elmquist JK, Coppari R, Balthasar N, Ichinose M, Lowell BB** 2005 Identifying hypothalamic pathways controlling food intake, body weight, and glucose homeostasis. J Comp Neurol 493:63–71
16. **Cowley MA, Smart JL, Rubinstein M, Cerdan MG, Diano S, Horvath TL, Cone RD, Low MJ** 2001 Leptin activates anorexigenic POMC neurons through a neural network in the arcuate nucleus. Nature 411:480–484
17. **Pinto S, Roseberry AG, Liu H, Diano S, Shanabrough M, Cai X, Friedman JM, Horvath TL** 2004 Rapid rewiring of arcuate nucleus feeding circuits by leptin. Science 304:110–115
18. **Wynne K, Stanley S, McGowan B, Bloom S** 2005 Appetite control. J Endocrinol 184:291–318
19. **Vrang N, Larsen PJ, Clausen JT, Kristensen P** 1999 Neurochemical characterization of hypothalamic cocaine-amphetamine-regulated transcript neurons. J Neurosci 19:1–8
20. **Freeman ME, Kanyicska B, Lerant A, Nagy G** 2000 Prolactin: structure, function, and regulation of secretion. Physiol Rev 80:1523–1631
21. **McCann SM, Lumpkin MD, Mizunuma H, Khorram O, Ottlecz J, Samson WK** 1984 Peptidergic and dopaminergic control of prolactin release. Trends Neurosci 7:127–131
22. **Levin MC, Sawchenko PE** 1993 Neuropeptide co-expression in the magnocellular neurosecretory system of the female rat: evidence for differential modulation by estrogen. Neurosci 54:1001–1018
23. **Bernardis LL, Bellinger LL** 1993 The lateral hypothalamic area revisited: neuroanatomy, body weight regulation, neuroendocrinology and metabolism. Neurosci Biobehav Rev 17:141–193
24. **Sawchenko PE, Swanson LW, Grzanna R, Howe PR, Bloom SR, Polak JM** 1985 Colocalization of neuropeptide Y immunoreactivity in brainstem catecholaminergic neurons that project to the paraventricular nucleus of the hypothalamus. J Comp Neurol 241:138–153
25. **Fox EA, Powley TL** 1985 Longitudinal columnar organization within the dorsal motor nucleus represents separate branches of the abdominal vagus. Brain Res 341:269–282
26. **Kozicz T** 2003 Neurons colocalizing urocortin and cocaine and amphetamine-regulated transcript immunoreactivities are induced by acute lipopolysaccharide stress in the Edinger-Westphal nucleus in the rat. Neurosci. 116:315–320
27. **Weitemier AZ, Ryabinin AE** 2005 Lesions of the Edinger-Westphal nucleus alter food and water consumption. Behav Neurosci 119:1235–1243
28. **Hornung JP** 2003 The human raphe nuclei and the serotonergic system. J Chem Neuroanat 26:331–343
29. **Jacobs BL, Martin-Cora FJ, Fornal CA** 2002 Activity of medullary serotonergic neurons in freely moving animals. Brain Res Rev 40:45–52
30. **Morrison SF** 2001 Differential control of sympathetic outflow. Am J Physiol Regul Integr Comp Physiol 281:R683–R698
31. **Nakamura K, Matsumura K, Kobayashi S, Kaneko T** 2005 Sympathetic premotor neurons mediating thermoregulatory functions. Neurosci Res 51:1–8
32. **Kase H., Iwahashi K, Nakanishi S, Matsuda Y, Yamada K, Takahashi M, Murakata C, Sato A, Kaneko M** 1987 K-252 compounds, novel and potent inhibitors of protein kinase C and cyclic nucleotide-dependent protein kinases. Biochem Biophys Res Commun 142:436–440
33. **Filipeanu CM, Brailoiu E, Le Dun S, Dun NJ** 2002 Urotensin-II regulates intracellular calcium in dissociated rat spinal cord neurons. J Neurochem 83:879–884
34. **Hou L, Wang X** 2001 PKC and PKA, but not PKG mediate LPS-induced CGRP release and $[Ca^{2+}]_i$ elevation in DRG neurons of neonatal rats. J Neurosci Res 66:592–600
35. **Santschi L, Reyes-Harde M, Stanton PK** 1999 Chemically induced, activity-independent LTD elicited by simultaneous activation of PKG and inhibition of PKA. J Neurophysiol 82:1577–1589
36. **Bylund DB, Ray-Prenger C** 1989 α-2A and α-2B adrenergic receptor subtypes: attenuation of cyclic AMP production in cell lines containing only one receptor subtype. J Pharmacol Exp Ther 251:640–644
37. **Daaka Y, Luttrell LM, Lefkowitz RJ** 1997 Switching of the coupling of the β2-adrenergic receptor to different G proteins by protein kinase A. Nature 390:88–91
38. **Luo X, Zeng W, Xu X, Popov S, Davignon I, Wilkie TM, Mumby SM, Muallem S** 1999 Alternate coupling of receptors to Gs and Gi in pancreatic and submandibular gland cells. J Biol Chem 274:17684–17690
39. **Dunn TA, Wang CT, Colicos MA, Zaccolo M, DiPilato LM, Zhang J, Tsien RY, Feller MB** 2006 Imaging of cAMP levels and protein kinase A activity reveals that retinal waves drive oscillations in second-messenger cascades. J Neurosci 26:12807–12815
40. **Jo SH, Leblais V, Wang PH, Crow MT, Xiao RP** 2002 Phosphatidylinositol 3-kinase functionally compartmentalizes the concurrent G(s) signaling during β2-adrenergic stimulation. Circ Res 91:46–53